



Published in final edited form as:

*Neuroreport*. 2008 May 7; 19(7): 703–709. doi:10.1097/WNR.0b013e3282fb8203.

## Residual functional connectivity in the split-brain revealed with resting-state fMRI

Lucina Q. Uddin<sup>1</sup>, Eric Mooshagian<sup>2</sup>, Eran Zaidel<sup>2,3</sup>, Anouk Scheres<sup>4</sup>, Daniel S. Margulies<sup>1</sup>, A. M. Clare Kelly<sup>1</sup>, Zarrar Shehzad<sup>1</sup>, Jonathan S. Adelstein<sup>1</sup>, F. Xavier Castellanos<sup>1</sup>, Bharat B. Biswal<sup>5</sup>, and Michael P. Milham<sup>1</sup>

<sup>1</sup>The Phyllis Green and Randolph C owen Institute for Pediatric Neuroscience, New York University Child Study Center, New York, NY 10016

<sup>2</sup>Department of Psychology, University of California Los Angeles, Los Angeles, CA 90095

<sup>3</sup>Brain Research Institute, University of California Los Angeles, Los Angeles, CA 90095

<sup>4</sup>Department of Psychology, University of Arizona, Tucson, AZ 85721

<sup>5</sup>Department of Radiology, University of Medicine and Dentistry of New Jersey, Newark, NJ 07101

### Abstract

Split-brain patients present a unique opportunity to address controversies regarding subcortical contributions to interhemispheric coordination. We characterized residual functional connectivity in a complete commissurotomy patient by examining patterns of low-frequency BOLD fMRI signal. Using independent components analysis (ICA) and region-of-interest (ROI) based functional connectivity analyses, we demonstrate bilateral resting state networks in a patient lacking all major cerebral commissures. Compared to a control group, the patient's interhemispheric correlation scores fell within the normal range for two out of three regions examined. Thus we provide evidence for bilateral resting state networks in a patient with complete commissurotomy. Such continued interhemispheric interaction suggests that, at least in part, cortical networks in the brain can be coordinated by subcortical mechanisms.

### Keywords

resting-state functional connectivity; DTI; laterality; commissurotomy; interhemispheric interaction

### Introduction

Patients who have undergone the “split-brain” operation to relieve severe intractable epilepsy provide a unique opportunity for cognitive neuroscientists to examine mechanisms of interhemispheric interaction, neural plasticity and compensatory reorganization. A somewhat surprising finding has been that aside from deficits visible under restricted testing conditions, these patients “show a remarkable absence of functional impairment in nearly all ordinary behavior” [1]. Numerous studies of split-brain patients have shown evidence for

---

Correspondence and requests for reprints should be addressed to: Lucina Q. Uddin or Michael P. Milham, New York University Child Study Center, 215 Lexington Avenue, 14<sup>th</sup> Floor, New York, NY 10016, Telephone: (212) 263-4673, Fax: (212) 263-4675, lucina.uddin@med.nyu.edu (L. Q. U.) or milham01@med.nyu.edu (M. P. M.).

**Disclosure:** The authors report no conflicts of interest.

continued interhemispheric transfer -- albeit degraded -- in the absence of cerebral commissures [2]. These patients can often transfer coarse perceptual visual information between the hemispheres [3]. The common assumption is that this is accomplished by subcortical pathways, which can compensate when low-level information transfer is required [3].

It is generally accepted that some interhemispheric transfer exists in these patients, yet our understanding of the coordination of processing between the split hemispheres remains limited. While some studies of typical interhemispheric coordination in neurologically intact participants suggest entirely cortico-cortical connections, others implicate subcortical contributions [4]. Efforts to differentiate between these possibilities have relied on measures of coherence as indexed by electroencephalogram (EEG), with conflicting findings. Coherence analyses of EEG have been used as an indicator of functional cortico-cortical connections, with coherence decreases thought to reflect decreased interhemispheric connectivity [4]. While some report residual coherence in human split-brains as well as in surgically callosotomized animals, supporting the idea of subcortical interhemispheric coordination [5], others report drastically reduced interhemispheric coherence post-operatively, suggesting that coherence is entirely mediated by cortico-cortical connectivity [6]. Unfortunately, EEG lacks the anatomic resolution required for studying specific networks. Recently developed functional connectivity measures applied to fMRI data provide an alternative method for studying interhemispheric coordination.

The discovery of resting-state functional connectivity in the motor system [7] has provided a new method for mapping major cortical networks. To date, coherent spontaneous fMRI activity has been used to identify attention systems [8], the default mode network [9], as well as several other resting state networks (RSNs) [10]. Resting state functional connectivity can also be used as a measure of interhemispheric coherence, with greater anatomic specificity than is possible with EEG. For example, a recent study has demonstrated that homologous regions of the anterior cingulate cortex in each hemisphere exhibit stronger correlations than non-homologous regions [11].

While the significance of these resting state networks is not yet fully understood, they are widely thought to reflect intrinsic functional architecture. In a recent review, it is suggested that these signals serve to organize and coordinate neuronal activity [12]. In support of a putative functional role in organizing and coordinating neural activity across distributed networks, it has been shown that low-frequency oscillations (< 0.1Hz) serve to synchronize activity in large-scale networks, while higher frequency oscillations modulate more local events [13]. Thus, current models in the literature point to organizational functional properties of resting-state networks.

Functional connectivity, whether measured by EEG or fMRI, is thought to reflect structural connectivity. Given the known structural connectivity existing between homologous regions in each cerebral hemisphere, cortical commissural fibers have long been purported to mediate the majority of interhemispheric interactions. In split-brain patients however, interhemispheric coordination, when it exists, must be mediated by extra-callosal pathways.

Here we used resting-state functional connectivity to establish the degree to which coordination of processing between the cerebral hemispheres can be supported by subcortical mechanisms. We used independent components analysis (ICA) and seed-based functional connectivity measures on fMRI data from a commissurotomy patient to test for the presence of continued patterns of bilateral connectivity in commonly observed resting state networks. This patient has been previously characterized using several behavioral assessments [14], and surgical reports verify completeness of the commissurotomy [1].

## Methods

### Participant: Patient N.G.

We tested patient N.G., a right-handed 74-year-old woman who underwent complete forebrain commissurotomy (single stage midline section of the anterior commissure, corpus callosum, hippocampal commissure, and massa intermedia) in 1963 to relieve intractable epilepsy. A complete case history is reported elsewhere [1]. Structural MRI images confirmed complete commissurotomy. This patient reportedly sustained greater pre-operative extra-callosal structural damage to the right hemisphere [15]. Behavioral testing in this patient has indicated some preserved interhemispheric interaction as indexed by various neuropsychological tests [15]. Pre- and post-operative full-scale IQ was 76, and 71 respectively. This study was approved by the IRB at the University of Arizona and New York University School of Medicine. Consent was obtained from the patient according to the Declaration of Helsinki, and she was compensated for her participation.

### Participants: Adult Controls

We used previously collected resting fMRI data from 42 adult subjects (20 females, average age =  $29.5 \pm 8.1$  years) as a reference group for comparison with data from N.G. in secondary analyses (described in Methods). Subsets of this dataset have been used in previous publications [11,16,17]. All participants in this sample were free of psychiatric disorders and had no history of head trauma. Subjects signed informed consent and received monetary compensation for participation. The study complied with Declaration of Helsinki and was IRB approved at New York University and the NYU School of Medicine.

### fMRI Acquisition Parameters: Patient N.G.

Data were acquired on a General Electric 3.0T HD Signa Excite scanner equipped with Optimized ACGD Gradients located at the University of Arizona. A resting scan of 6 minute duration was acquired during which the subject received no visual stimuli (TR = 2000ms; TE = 25ms; Flip angle = 90, 40 slices, matrix 64×64; FOV = 230mm; acquisition voxel size = 3×3×4mm). An additional functional scan was acquired (TR = 2000ms; TE = 25ms; Flip angle = 90, 40 slices, matrix 64×64; FOV = 230mm; acquisition voxel size = 3×3×3), during which the subject was asked to complete a fingertapping task, but was unable to comply with instructions. This functional scan was thus equivalent to a resting scan. A T1-weighted anatomical image was acquired for registration purposes and to confirm complete commissurotomy (MP-RAGE, TR = 2500ms; TE = 4.35ms; TI = 900ms; Flip angle = 8; 176 slices; FOV = 256mm). A 25-direction DTI sequence was also acquired in order to rule out the existence of residual callosal fibers (TR = 13000ms; TE = 72.1ms; Flip angle = 90; matrix 128×128; FOV = 25.6cm; 3mm slices).

### fMRI Acquisition Parameters: Adult Controls

Functional images were acquired on a Siemens Allegra 3-Tesla scanner located at New York University using an EPI gradient echo sequence (TR = 2000ms; TE = 25ms; Flip angle = 90, 39 slices, matrix 64×64; FOV = 192mm; acquisition voxel size 3×3×3mm) while subjects were instructed to rest with eyes open. For each participant, 197 contiguous EPI functional volumes were acquired, resulting in a 6 min 38 s scan. During this scan, the word “Relax” was projected in white font against a black background. A T1-weighted anatomical image was also acquired for registration purposes (MP-RAGE, TR = 2500ms; TE = 4.35ms; TI = 900ms; Flip angle = 8; 176 slices; FOV = 256mm).

## Data Analysis

The functional scans collected from patient N.G. were initially analyzed using FSL's MELODIC ICA (<http://www.fmrib.ox.ac.uk/fsl/>). ICA is a model-free approach for analyzing functional neuroimaging data that decomposes a 2d (time  $\times$  voxels) data matrix into a set of timecourses and associated spatial maps, which describe temporal and spatial characteristics of underlying hidden signals, or components [18]. ICA was used as a primary approach to objectively identify resting state networks, as described below. Subsequently, those networks readily identifiable with ICA were further characterized using a seed-based approach that has become standard in the field of resting-state functional connectivity [9,11,12] to detect interregional temporal correlations in fMRI signal fluctuations (see Table 1).

## Independent Components Analysis

Data were analyzed using MELODIC (Multivariate Exploratory Linear Decomposition into Independent Components) Version In(11), part of FSL (FMRIB's Software Library). The two functional scans were combined for this analysis to increase power. Pre-processing of the data was applied as follows: masking of non-brain voxels; voxel-wise de-meaning of the data; normalization of the voxel-wise variance. Pre-processed data were whitened and projected into a 75-dimensional subspace using probabilistic Principal Component Analysis where the number of dimensions was estimated using the Laplace approximation to the Bayesian evidence of the model order [19]. The whitened observations were decomposed into a set of time-courses and spatial maps by optimizing for non-Gaussian spatial source distributions using a fixed-point iteration technique. Estimated Component maps were divided by the standard deviation of the residual noise and thresholded by fitting a mixture model to the histogram of intensity values [19]. From this analysis, components were visually inspected to identify those corresponding to several previously identified resting state networks [10]. Three additional bilateral networks were also observed. These were less reliably related to previously characterized networks, likely reflecting individual variability, possible reorganization in this patient, or effects of age, and have thus been excluded from the current analysis.

## Seed-based functional connectivity

For this analysis, the first resting-state scan was used. We created spherical "seed" ROIs (10  $3 \times 3 \times 3$  mm voxels, volume =  $270 \text{ mm}^3$ ) using Talairach coordinate locations from previous work [10] (Table 1). These Talairach coordinates were converted to MNI space using the algorithm implemented in the Matlab script `tal2mni.m` (<http://imaging.mrc-cbu.cam.ac.uk/imaging/MniTalairach>). Two ROIs for each RSN were used to extract an average hemodynamic timeseries for each network in each hemisphere by applying each ROI mask to the preprocessed timeseries, and averaging across all voxels within the ROI. We then carried out separate multiple regression analyses (using the GLM as implemented in FSL's FEAT) for each set of seeds, with the seed timeseries regressors and nuisance covariates (global signal, cerebrospinal fluid, white matter), as well as 6 motion regressors. The global signal, which reflects a combination of physiological processes (such as cardiac and respiratory fluctuations) and scanner drift, was included in the GLM to minimize the influence of such factors [17]. Each ROI timeseries was orthogonalized with respect to the nuisance covariates, to the 6 motion regressors, and to 19 artifact components identified by ICA. These methods are described in detail in a recent publication from our group [11], and are becoming standard practice in analysis of resting-state data [12].

## Interhemispheric correlations

In order to provide a quantitative comparison of interhemispheric connectivity between N.G. and the neurologically intact control group, for each seed, we calculated interhemispheric correlation scores for each participant. The hemodynamic timeseries for each coordinate listed in Table 1 was extracted for each subject and a correlation was computed between the timeseries from the left hemisphere and the timeseries from the homologous coordinate in the right hemisphere. Results from these comparisons are presented in Table 2 and Figure 3.

## Diffusion Tensor Imaging

Fractional anisotropy (FA) maps thresholded at 0.25 are presented in Figure 4. A program implemented in MATLAB was used to calculate the Diffusion Tensor. For  $S_0$  and  $S_i$  representing the signal intensity with  $b = 0$ , and the signal intensity in the  $i^{\text{th}}$  direction and  $b =$  diffusion weighting,  $Y = [\ln(S_0/S_1)/b, \ln(S_0/S_2)/b, \dots, \ln(S_0/S_M)/b]^T$ . The noise in the data for each acquisition can then be expressed as  $Y = Hd + \eta$ , with  $d = H^{-1}Y$ . In cases with more than six directions, the  $H$  matrix is not a square matrix, so it is not possible to calculate the inverse  $H^{-1}$ . However, psuedoinverse  $H^\circ$  can be calculated such that  $H^\circ H = I_{6 \times 6}$ .  $H^\circ H = (H^T H)^{-1} H^T$ . The Tensor  $[\lambda_1, \lambda_2, \lambda_3]$  = diagonalization of  $d$ . Fractional Anisotropy was calculated as:  $FA = \sqrt{3[(\lambda_1 - \langle \lambda \rangle)^2 + (\lambda_2 - \langle \lambda \rangle)^2 + (\lambda_3 - \langle \lambda \rangle)^2]} / \sqrt{2(\lambda_1^2 + \lambda_2^2 + \lambda_3^2)}$ . As can be seen from the map, no residual commissural fibers exist in this patient.

## Results

The ICA analysis revealed two notable bilateral components (Fig 1). The first appeared to be the posterior portion of what has come to be known as the default mode network [20], comprising posterior cingulate and lateral parietal cortices. The second closely matched a posterior network characterized by involvement of occipital cortex referred to in the literature as RSN 1 [10].

The seed-based functional connectivity analysis confirmed that the two networks revealed using ICA were indeed present bilaterally. Networks correlated with each of the seed ROIs are shown in Fig.2. For seeds placed in various left hemisphere (LH) regions (Fig. 2a), a strongly bilateral network was revealed by the regression analyses. A similar, though weaker, bilateral pattern emerged for right hemisphere (RH) seeds (Fig. 2b). It is likely that pre-operative structural damage to the RH in this patient contributes to the weaker functional connectivity from right to left regions. Results for a comparison of N.G.'s interhemispheric correlation scores with scores from 42 neurologically intact participants are shown in Fig. 3. Table 2 summarizes the average and standard deviation of interhemispheric correlation scores for the control subjects and for patient N.G. For two out of three of the coordinates examined, N.G. fell well within the standard deviation (Table 2).

## Discussion

In summary, we assessed interhemispheric coordination in a commissurotomy patient using ICA and seed ROI-based functional connectivity measures, both of which revealed a surprisingly high degree of bilaterality. Such interhemispheric coordination in the absence of all major commissures, including the corpus callosum, suggests that the low-frequency BOLD signal that gives rise to large-scale resting state networks can be coordinated subcortically. Behavioral analyses have shown large individual differences in interhemispheric transfer among split-brain patients [2]. The patient studied here shows remarkably spared visual transfer. Specifically, she is able to match meaningful as well as nonsense shapes of varying complexity, as well as letter shapes across the vertical meridian, but not letter names or facial identity [21]. This is consistent with the existence of strong

bilateral connectivity in primary visual cortex (RSN 1), as demonstrated here. Additionally, this patient shows preserved bilaterality in regions comprising the default mode network [20]. This network exhibits high baseline levels of activity that is attenuated during externally-oriented cognitive tasks, and is thought to be involved in a variety of self-referential and social cognitive functions [22]. Recent work has shown decreases in connectivity between the anterior and posterior portions of this network with age [23], consistent with our data.

The fact that specific resting state networks maintain bilateral presence after complete commissurotomy strongly suggests that their coordination is subcortical in origin, post-surgery. It remains possible that in the intact brain, a dual mechanism exists such that both cortical and subcortical mechanisms work to coordinate networks, but the persistence of bilateral networks in our commissurotomy patient suggests that commissural connections are not the only fibers involved in maintaining interhemispheric coordination and coherence. It is likely that in the intact brain, commissural connections do exert a greater influence, but in the absence of such connections, the subcortical mechanism takes over. Such a dual mechanism model is consistent with studies demonstrating greater contributions of subcortical structures during sleep than waking states [4]. Future work in neuroimaging of acutely post-operative patients will help to clarify this issue, and assess compensatory reorganization unfolding over time.

Understanding the mechanisms of interhemispheric coordination has been a central problem in the field of cognitive neuroscience. Given the vast literature on compromised interhemispheric coordination in commissurotomy patients, it has long been asserted that the commissural fibers are necessary for transfer of complex cognitive information [24]. However, in this and other split-brain patients, several investigators have noted that transfer of some types of visual information is usually spared [21]. The commonly accepted explanation for residual interhemispheric coordination in split-brain patients is that subcortical pathways suffice to transfer simple visual information [3,21,25]. Our data are consistent with the claim that such subcortical connections operate when the corpus callosum is surgically severed. We reasoned that if such subcortical pathways exist, then they should be detectable using the methods of resting-state functional connectivity. Here we have demonstrated just such connectivity in a commissurotomy patient.

## Limitations

A limitation of the current study is the lack of task-related activation data. Unfortunately, due to the patient's age and reduced motor ability, we were unable to collect additional data during a task paradigm (for example, finger-tapping) that would have allowed us to address the interesting question of functional connectivity during task performance after complete commissurotomy. However, resting-state fMRI is increasingly used to examine network integrity in clinical populations for which task-based paradigms are difficult to implement. One of the advantages of the resting-state approach is that it is "cognitively unbiased", or independent of task performance, yet is related in meaningful ways to cognition and behavior [16].

Another limitation is the use of two different scanners (General Electric 3.0T HD Signa Excite, and Siemens Allegra 3-Tesla) for collection of data from the patient and normal adult control group, respectively. This was unavoidable due the geographical location of the patient, and precludes further direct comparison of data between the patient and control population.

Finally, our data represents the brain of one individual, and thus awaits replication by studies on other comparable patients. Unfortunately, such patients are rare as the complete



commissurotomy surgery as treatment for intractable epilepsy has been largely replaced by pharmacological interventions.

## Conclusion

We used two different methods, ICA and seed-based analyses, to demonstrate functional connectivity between homologous regions with a high degree of anatomic specificity, in the two disconnected cerebral hemispheres. This is the first neuroimaging evidence of bilateral resting state networks in a patient with no cortical commissural fibers. Our findings suggest that resting state networks in the brain are at least in part subcortically coordinated, and that the sparing of information transfer between the hemispheres of split-brain patients is mirrored in the specific bilateral resting state networks.

## Supplementary Material

Refer to Web version on PubMed Central for supplementary material.

## Acknowledgments

We would like to thank N.G. and her family for their willing participation. We gratefully acknowledge Scott Squire and Matt Hoptman for technical support.

### Funding

Stavros S. Niarchos Foundation; National Institute of Mental Health (5R21MH066393, 5T32MH067763); Leon Lowenstein Foundation to F.X.C. National Institute of Health (NS20187) to E.Z.

## References

1. Bogen JE, Fisher ED, Vogel PJ. Cerebral Commissurotomy: A Second Case Report. *Journal of the American Medical Association*. 1965; 194:1328–1329. [PubMed: 4954563]
2. Zaidel, E.; Iacoboni, M.; Zaidel, D.; Bogen, J. The callosal syndromes. In *Clinical Neuropsychology*. Heilman, KM.; Valenstein, E., editors. Oxford University Press; New York: 2003. p. 347-403.
3. Funnell MG, Corballis PM, Gazzaniga MS. Insights into the functional specificity of the human corpus callosum. *Brain*. 2000; 123(Pt 5):920–926. [PubMed: 10775537]
4. Leocani L, Comi G. EEG coherence in pathological conditions. *J Clin Neurophysiol*. 1999; 16(6): 548–555. [PubMed: 10600022]
5. Corsi-Cabrera M, Trias G, Guevara MA, Haro R, Hernandez A. EEG interhemispheric correlation after callosotomy: one case study. *Percept Mot Skills*. 1995; 80(2):504–506. [PubMed: 7675581]
6. Nielsen TA, Montplaisir J. Is interhemispheric connectivity reduced after callosotomy? A critique. *Percept Mot Skills*. 1996; 83(1):348–350. [PubMed: 8873213]
7. Biswal B, Yetkin FZ, Haughton VM, Hyde JS. Functional connectivity in the motor cortex of resting human brain using echo-planar MRI. *Magn Reson Med*. 1995; 34(4):537–541. [PubMed: 8524021]
8. Fox MD, Corbetta M, Snyder AZ, Vincent JL, Raichle ME. Spontaneous neuronal activity distinguishes human dorsal and ventral attention systems. *Proc Natl Acad Sci U S A*. 2006; 103(26): 10046–10051. [PubMed: 16788060]
9. Greicius MD, Krasnow B, Reiss AL, Menon V. Functional connectivity in the resting brain: a network analysis of the default mode hypothesis. *Proc Natl Acad Sci U S A*. 2003; 100(1):253–258. [PubMed: 12506194]
10. De Luca M, Beckmann CF, De Stefano N, Matthews PM, Smith SM. fMRI resting state networks define distinct modes of long-distance interactions in the human brain. *Neuroimage*. 2006; 29(4): 1359–1367. [PubMed: 16260155]

11. Margulies DS, Kelly AM, Uddin LQ, Biswal BB, Castellanos FX, Milham MP. Mapping the functional connectivity of anterior cingulate cortex. *Neuroimage*. 2007; 37(2):579–588. [PubMed: 17604651]
12. Fox MD, Raichle ME. Spontaneous fluctuations in brain activity observed with functional magnetic resonance imaging. *Nat Rev Neurosci*. 2007; 8(9):700–711. [PubMed: 17704812]
13. Buzsaki G, Draguhn A. Neuronal oscillations in cortical networks. *Science*. 2004; 304(5679):1926–1929. [PubMed: 15218136]
14. Zaidel, E.; White, H.; Sakurai, E.; Banks, W. Hemispheric locus of lexical congruity effects: Neuropsychological reinterpretation of psycholinguistic results. In: Chiarello, C., editor. *Right Hemisphere Contributions to Lexical Semantics*. Springer; New York: 1988. p. 71-88.
15. Campbell AL Jr. Bogen JE, Smith A. Disorganization and reorganization of cognitive and sensorimotor functions in cerebral commissurotomy. Compensatory roles of the forebrain commissures and cerebral hemispheres in man. *Brain*. 1981; 104(3):493–511. [PubMed: 7272712]
16. Clare Kelly AM, Uddin LQ, Biswal BB, Castellanos FX, Milham MP. Competition between functional brain networks mediates behavioral variability. *Neuroimage*. 2008; 39(1):527–537. [PubMed: 17919929]
17. Uddin LQ, Clare Kelly AM, Biswal BB, Xavier Castellanos F, Milham MP. Functional connectivity of default mode network components: Correlation, anticorrelation, and causality. *Hum Brain Mapp*. 2008
18. Beckmann CF, DeLuca M, Devlin JT, Smith SM. Investigations into resting-state connectivity using independent component analysis. *Philos Trans R Soc Lond B Biol Sci*. 2005; 360(1457):1001–1013. [PubMed: 16087444]
19. Beckmann CF, Smith SM. Probabilistic independent component analysis for functional magnetic resonance imaging. *IEEE Trans Med Imaging*. 2004; 23(2):137–152. [PubMed: 14964560]
20. Raichle ME, MacLeod AM, Snyder AZ, Powers WJ, Gusnard DA, Shulman GL. A default mode of brain function. *Proc Natl Acad Sci U S A*. 2001; 98(2):676–682. [PubMed: 11209064]
21. Eviatar Z, Zaidel E. Letter matching within and between the disconnected hemispheres. *Brain Cogn*. 1994; 25(1):128–137. [PubMed: 8043263]
22. Uddin LQ, Iacoboni M, Lange C, Keenan JP. The self and social cognition: the role of cortical midline structures and mirror neurons. *Trends Cogn Sci*. 2007
23. Damoiseaux JS, Beckmann CF, Smith SM, et al. The effects of normal aging on resting state networks. *Organization for Human Brain Mapping*. 2007
24. Zaidel, E. Interhemispheric transfer in the split brain: Long-term status following complete cerebral commissurotomy. In: Davidson, RH.; Hugdahl, K., editors. *Brain Asymmetry*. MIT Press; Cambridge: 1994. p. 491-532.
25. Clarke JM, Zaidel E. Simple reaction times to lateralized light flashes. Varieties of interhemispheric communication routes. *Brain*. 1989; 112(Pt 4):849–870. [PubMed: 2775994]



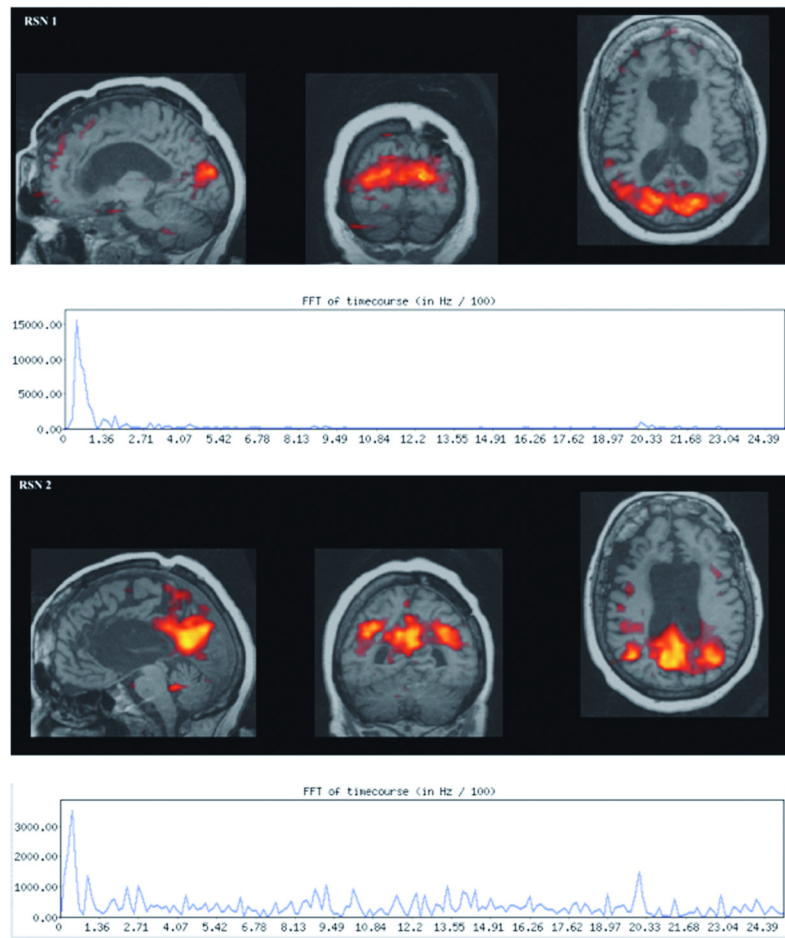


**Fig. 1. Resting State Networks identified using ICA**

Two components were identified by ICA. These components had Fast Fourier transform timecourses consistent with known resting state networks (< 0.1 Hz).

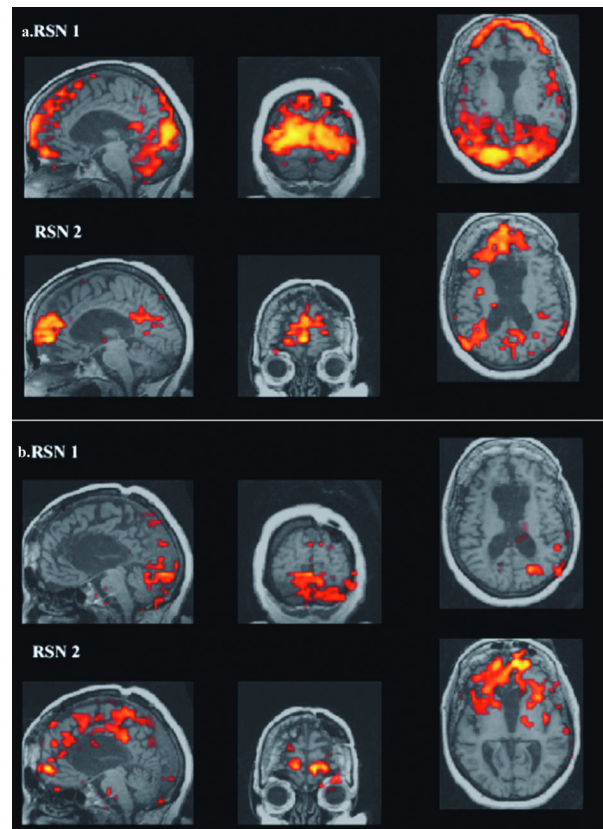


**Fig. 2. Networks correlated with seeds in the LH (a) and RH (b)**  
**a. Left Seed ROIs.** Seeds placed in the LH (see Table 1 for coordinates) revealed bilateral patterns of connectivity.  
**b. Right Seed ROIs.** Seeds placed in the homologous RH regions also revealed bilateral connectivity, though weaker.

### Range of Interhemispheric Correlation Scores

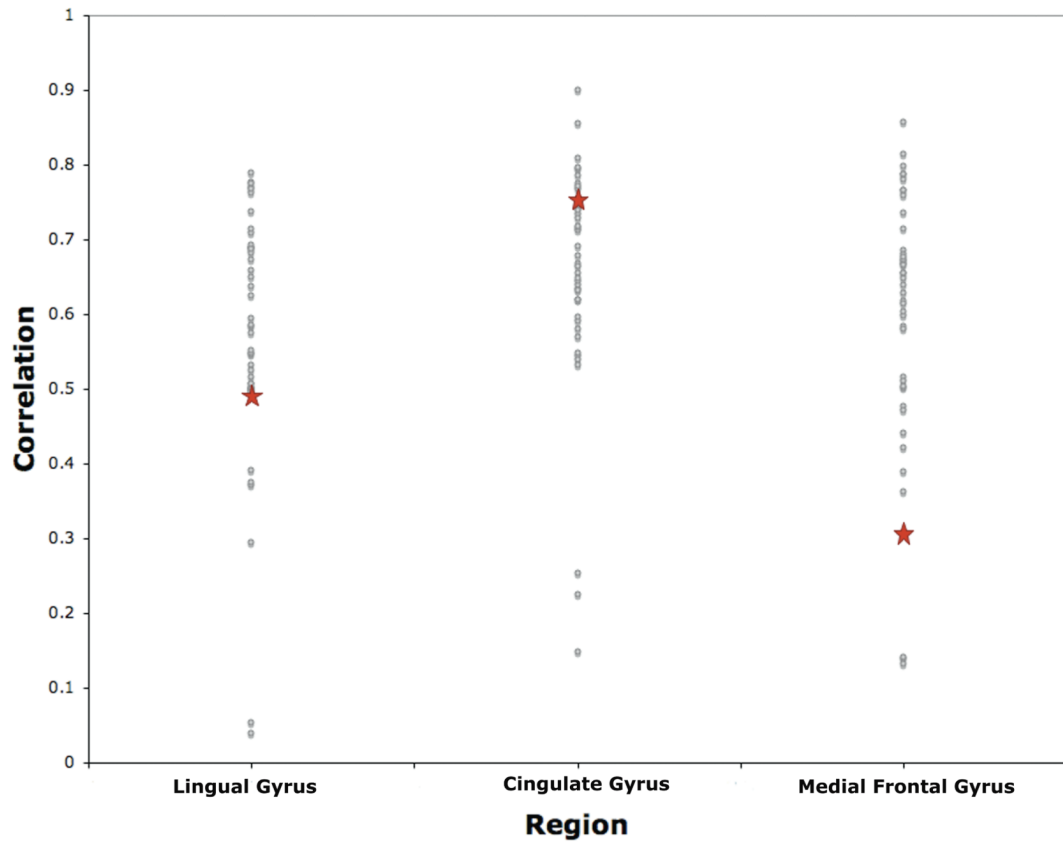


**Fig. 3. Interhemispheric correlation scores**

Interhemispheric correlation scores from 42 neurologically intact control participants show a wide distribution. Scores for patient N.G. (red stars) fall within the normal range for 2 out of 3 of the regions examined.

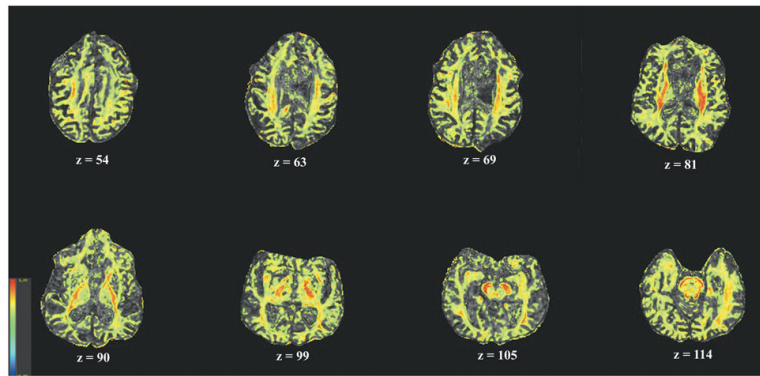


**Figure 4. Diffusion Tensor Imaging**

Fractional anisotropy maps from patient N.G. demonstrate completeness of commissurotomy. No residual interhemispheric fibers can be detected.

**Table 1**  
**MNI Coordinates of seed ROI locations**

| Network | Region                    | X   | y    | z  |
|---------|---------------------------|-----|------|----|
| RSN 1   | L. Middle occipital gyrus | -22 | -88  | 17 |
|         | R. Middle occipital gyrus | 22  | -76* | 17 |
|         | L. Lingual gyrus          | -8  | -80  | -8 |
|         | R. Lingual gyrus          | 8   | -80  | -8 |
| RSN 2   | L. Cingulate gyrus        | -8  | -54  | 27 |
|         | R. Cingulate gyrus        | 8   | -54  | 27 |
|         | L. Medial frontal gyrus   | -8  | 56   | 0  |
|         | R. Medial frontal gyrus   | 8   | 56   | 0  |

\* This coordinate was placed slightly more medially due to accommodate artifact in the scan.

**Table 2**  
**Interhemispheric correlation scores**

|                             | Middle Occipital Gyrus | Cingulate Gyrus | Medial Frontal Gyrus |
|-----------------------------|------------------------|-----------------|----------------------|
| <b>Patient N.G.</b>         | 0.4960                 | 0.7384          | 0.3070               |
| <b>Controls (Mean)</b>      | 0.5776                 | 0.6552          | 0.5982               |
| <b>Controls (Std. Dev.)</b> | 0.1707                 | 0.1537          | 0.1767               |